Available online at www.sciencedirect.com
SCIENCE DIRECT
Biochimica et Biophysica Acta 1708 (2005) 362 – 366
BIOCHIMICA ET BIOPHYSICA ACTA
BBA
http://www.elsevier.com/locate/bba

Coherent phase microscopy in cell biology: Visualization of metabolic states

Vladimir P. Tychinsky[a], Alexander V. Kretushev[a], Tatyana V. Vyshenskaya[b], Alexander N. Tikhonov[b,*]

[a]*Moscow State Institute for Radioengineering, Electronics and Automation, prosp. Vernadskogo 78, 119454 Moscow, Russia*
[b]*Faculty of Physics, M.V. Lomonosov Moscow State University, 119992 Moscow, Russia*

Received 19 February 2005; accepted 27 April 2005
Available online 23 May 2005

Abstract

Visualization of functional properties of individual cells and intracellular organelles still remains an experimental challenge in cell biology. The coherent phase microscopy (CPM) provides a convenient and non-invasive tool for imaging cells and intracellular organelles. In this work, we report results of statistical analysis of CPM images of cyanobacterial cells (*Synechocystis* sp. PCC 6803) and spores (*Bacillus licheniformis*). It has been shown that CPM images of cyanobacterial cells and spores are sensitive to variations of their metabolic states. We found a correlation between one of optical parameters of the CPM image ('phase thicknesses' Δh) and cell energization. It was demonstrated that the phase thickness Δh decreased after cell treatment with the uncoupler CCCP or inhibitors of electron transport (KCN or DCMU). Statistical analysis of distributions of parameter Δh and cell diameter d demonstrated that a decrease in the phase thickness Δh could not be attributed entirely to a decrease in geometrical sizes of cells. This finding demonstrates that the CPM technique may be a convenient tool for fast and non-invasive diagnosis of metabolic states of individual cells and intracellular organelles.

Keywords: Coherent phase microscopy; Cyanobacteria; Spores; Membrane potential

1. Introduction

New microscopes and image-processing software allow precise quantitative analysis of cells and intracellular structures [1–5]. Confocal [6] and fluorescence [7] microscopes are usually used for monitoring biological processes in live specimens. Fluorescence dyes [8,9] and green fluorescent proteins (GFP) [10–12] are often served as molecular probes for measuring the local physical–chemical characteristics (e.g., membrane potential [13,14] or intracellular pH [15,16]) in different domains of the living cell. However, the non-invasive monitoring of metabolic states in individual cells or energy transducing organelles (mitochondria and chloroplasts) still remains an experimental challenge. There are several indications [17–20] that coherent phase microscopy (CPM) provides one of the most sensitive methods for the non-invasive diagnosis of metabolic states in mitochondria [18,19] and chloroplasts [20]. A CPM image of a specimen represents a 3D plot of the optical path difference (or "phase thickness") measured in the direction of a laser beam (Z-axis). Any thin transparent microobject may be regarded as a structured optically inhomogeneous medium, which results in deformation of the laser beam wavefront in the image plane (x,y). The CPM method allows the visualization of an object as a 3D plot of the optical path difference. The optical path difference $h(x,y)$ in a certain point (x,y) is proportional to the difference between the Z-projections of averaged refractive indices of an object, $n(x,y,z)$, and that of an immersion solution n_o ($n_o \cong 1.33$) onto the direction of a laser beam. Spatial and temporal

Abbreviations: CPM, coherent phase microscopy; DCMU, 3-(3,4-dichlorophenyl)-1,1-dimethylurea; CCCP, carbonylcyanide-3-chlorophenyl hydrazone

* Corresponding author. Tel.: +7 95 9392973; fax: +7 95 9391195.
E-mail address: an_tikhonov@newmail.ru (A.N. Tikhonov).

0005-2728/$ - see front matter © 2005 Elsevier B.V. All rights reserved.
doi:10.1016/j.bbabio.2005.04.002

resolutions of the objects provided by coherent phase microscope are about 100 nm and 1 ms, respectively [17]. Advanced modification of the CPM technique, dynamic phase microscopy, allows spatial and temporal resolution to be improved by measuring the frequency spectrum and other parameters of Δh fluctuations, which reflect dynamic properties of an object [20].

Here, we first report results of statistical analysis of CPM images of individual cells of the cyanobacterium *Synechocystis* sp. PCC 6803 and spores of *Bacillus licheniformis*. We found that the phase thickness of CPM images correlated with cell energization. This phenomenon allows identifying metabolic states of single cells by the CPM method.

2. Materials and methods

2.1. Optical measurements

CPM images of individual cells were obtained with a coherent phase microscope "Airyscan" [17], which is the modified Linnik-type microinterferometer with a He–Ne laser ($\lambda = 633$ nm) as a light source. Fig. 1 shows the layout of a coherent phase microscope "Airyscan" used in our work. A sample (a drop of cell suspension) was placed onto the quevette (a polished silicon plate with a cover glass fixed by 20 μm over the substrate). Measurements of the phase thicknesses $\Delta h(x,y)$ in different points (x,y) of a sample were performed by means of linear periodic modulation of the reference wave phase with a mirror attached to a piezoelectric actuator. Spatial and temporal resolutions were 100 nm and 1 ms, respectively. An LI-620 coordinate-sensitive photodetector (dissector image tube, "Electron" Inc.) and an electronic unit were used for recording the interference signal and its analog-to-digital conversion to the phase thickness value. The field of view of the lens (Olimpus 50*/0.75) was 20×20 μm. All measurements were performed at 20 °C. Duration of a sample exposure to laser light was usually about 1–2 min.

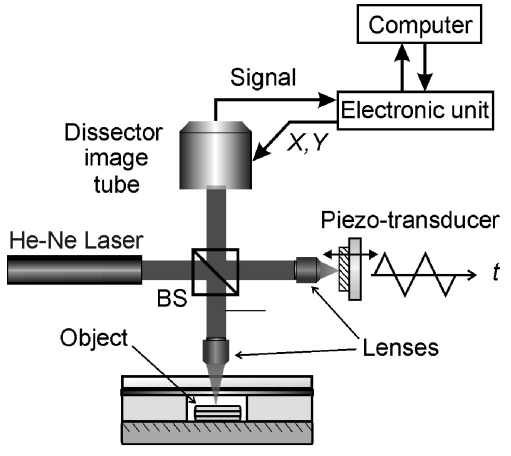

Fig. 1. Schematic view of the apparatus for cell imaging. Layout of the coherent phase microscope (CPM).

2.2. Cyanobacteria

Wild-type cells of *Synechocystis* sp. PCC 6803 were grown in BG-11 medium as described earlier [21]. Cells from liquid cultures in the late exponential phase of grows were harvested by centrifugation and washed once with 50 mM HEPES–NaOH buffer, pH 7.5. Cells were stored at room temperature (20–22 °C) at a chlorophyll concentration of 1 mg/ml. To inhibit electron transport in cyanobacteria, cells were suspended in solutions containing either 100 μM 3-(3,4-dichlorophenyl)-1,1-dimethylurea (DCMU, an inhibitor of photosystem II), or 8 mM KCN (an inhibitor of heme-containing proteins). Carbonylcyanide m-chlorophenylhydrazone (CCCP, 160 μM) was used as a protonophore uncoupler dissipating the transmembrane proton gradient.

2.3. Spores

Spores *Bacillus licheniformis* [22] were suspended in distilled water and then placed onto the microscope quevette for CPM measurements. Inactivated spores were obtained by heat treatment of spores for 30 min at 120 °C.

3. Results and discussion

3.1. Cyanobacteria Synechocystis sp. PCC 6803

3.1.1. Visualization of single cells by CPM method

Fig. 2 shows a typical pattern of the cross-section of the CPM image of a single cyanobacterial cell (*Synechocystis* sp. PCC 6803). Parameters d and Δh were determined as the half-width and the height of the phase thickness profile $h(x)$ corresponding to the cross-section of a CPM image through the cell center along the line $y = \text{const}$. The most informative parameters of an object revealed by the CPM method are the phase thickness Δh and cross-section dimension d (Fig. 2). Fig. 3a compares typical patterns of CPM images (topograms) of two cyanobacterial cells; one from suspension of normal (control) cells and another one from suspension of cells treated with an inhibitor, KCN. In the plane (x,y), the CPM images of these cells are close to a circle (Fig. 3b, c). It is noteworthing that control sample is characterized by higher phase thickness Δh than KCN-treated cell (Fig. 3a). This indicates that optical parameter Δh can be sensitive to the functional state of cyanobacterial cell. A phase thickness $\Delta h(x,y)$ in a point (x,y) depends on the product of the local refractive index of the object, $\Delta n(x,y)$, and its geometrical size in Z-direction (along laser beam) [17]. However, statistical analysis of distributions of optical parameters Δh and d demonstrate (Figs. 4 and 5) that a decrease in the phase thickness Δh caused by cell treatment with inhibitors

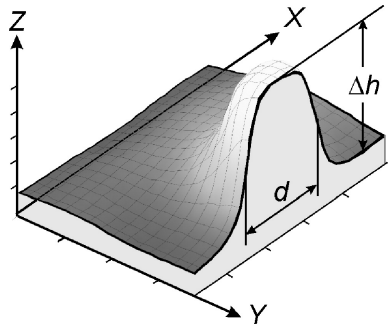

Fig. 2. A cross-section of the CPM image of a single cyanobacterial cell (*Synechocystis* sp. PCC 6803). Parameters d and Δh were determined as the half-width and the height of the phase thickness profile $h(x)$ corresponding to the cross-section of a CPM image through the cell center along the line $y=$const.

cannot be attributed entirely to a decrease in geometrical sizes of cells.

3.1.2. Statistical analysis of optical parameters d and Δh

Optical parameters d and Δh characterizing the topogram of a single cell are scattered within a population of cells. Fig. 4 compares the plots of parameter Δh versus a cell diameter d for populations of control cyanobacterial cells (Fig. 4a) and cells treated either with the uncoupler CCCP (Fig. 4b) or inhibitors of electron transport, KCN (Fig. 4c) or DCMU (Fig. 4d). We found that statistically significant correlation between parameters Δh and d was observed neither in control (Fig. 4a) nor in inhibitor-treated cells (Fig. 4b–d). One can see, however, that the treatments of cyanobacterial cells with CCCP, KCN or DCMU, which

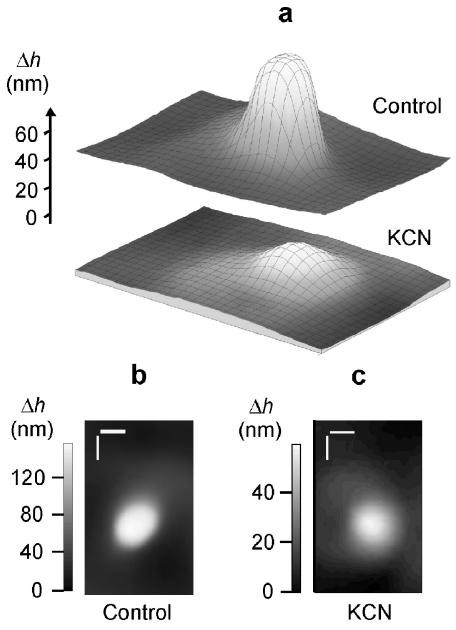

Fig. 3. Experimental results showing the influence of KCN (8 mM) on a CPM image on cyanobacterium. (a) Typical patterns of 3D CPM images of control and KCN-treated cells. (b, c) 2D CPM images of control (b) and KCN-treated (c) cells.

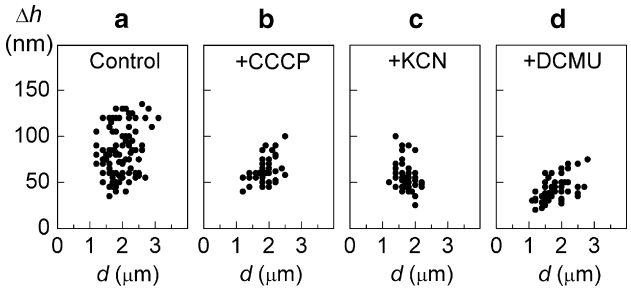

Fig. 4. Experimental results showing the lack of correlation between optical parameters Δh and d characterizing 3D CPM images of cyanobacteria *Synechocystis* sp. PCC 6803. Plots Δh versus d for populations of control cells (a, $N=115$), CCCP-treated cells (b, $N=51$), KCN-treated cells (c, $N=52$) and DCMU-treated cells (d, $N=56$).

suppressed metabolic activity of cyanobacteria, caused a decrease in the phase thickness Δh. This result demonstrates that a decrease in the phase thickness Δh, induced by inhibition of electron transport processes (additions of KCN or DCMU) or de-energization of cells by CCCP cannot be accounted for by mere decrease in cell size.

Fig. 5a compares histograms of cell distributions over diameter d, $P(d)$, in populations of control cyanobacteria and cells treated with protonophore inhibitor CCCP or inhibitors of electron transport (KCN or DCMU). Control cells are characterized by slightly broader profile $P(d)$ than inhibited cells. In the meantime, average diameters $\langle d\rangle$ in control and inhibitor-treated cells were virtually the same, $\langle d\rangle \approx 1.8-1.9$ μm, which is close to typical size of cyanobacterium *Synechocystis* sp. PCC 6803 [23]. This is not the case, however, if we consider the distributions of cells over the phase thickness Δh, $P(\Delta h)$ (Fig. 5b). In population of control cells, the profile $P(\Delta h)$ is much more broader than in inhibited cells. Contrary to uncoupler- or inhibitor-treated cells,

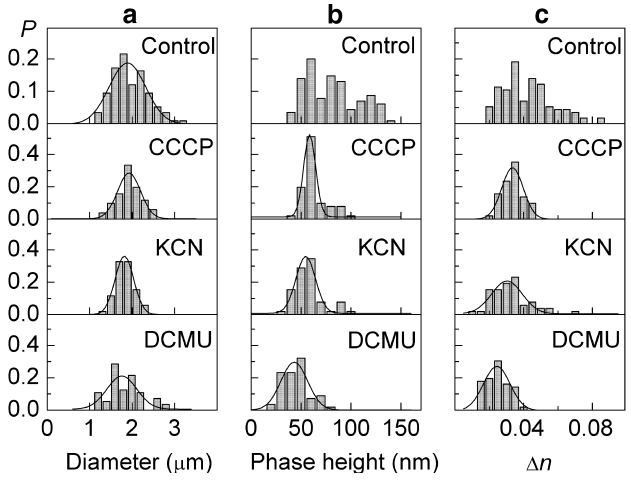

Fig. 5. Histograms demonstrating cell distribution over diameter d (a), phase thickness Δh (b), and dimensionless parameter $\Delta n=\Delta h/d$ (c, averaged refractive index) for populations of control cells ($N=115$) and cells treated with CCCP ($N=51$), KCN ($N=52$) or DCMU ($N=56$), as indicated.

control cyanobacteria reveal the co-existence of subpopulations with relatively low ($\Delta h \approx 40-80$ nm) and relatively high ($\Delta h \approx 80-140$ nm) phase thickness. These subpopulations could be attributed to cells with different metabolic activities. Actually, the additions of CCCP, KCN or DCMU, which suppress bioenergetic processes in cyanobacteria, caused an essential narrowing of the profile $P(\Delta h)$. The treatment of cyanobacteria with CCCP, KCN or DCMU shifted the distribution $P(\Delta h)$ toward lower values of Δh. In the presence of uncoupler CCCP, which dissipated the transmembrane proton gradient [24], the distribution $P(\Delta h)$ had one extreme at $\Delta h \approx 55-60$ nm. For cells treated with KCN, which inhibits electron transfer at different sites of the respiratory and photosynthetic electron transport chains [24,25], we observed one extreme at $\Delta h \approx 55$ nm. In the presence of DCMU (an inhibitor of photosynthetic electron transport [25]), the distribution $P(\Delta h)$ also had one peak at $\Delta h \approx 45$ nm. Thus, when bioenergetic processes in cyanobacteria were suppressed, either due to dissipation of the proton gradient or inhibition of electron transport, we did not observe subpopulations with a high phase thickness ($\Delta h \approx 80-140$ nm) that were present in control cyanobacteria.

Another evidence for a correlation between cell metabolic activity and Δh value came from our experiments on prolonged exposure of cells to measuring laser beam. Usually, to obtain CPM image, each cell was illuminated for less than 1–2 min. However, with extension of cell exposure to light (up to 20 min), we observed a certain decrease in the number of cells with high values of parameter Δh (data not shown). This result can be explained by photoinhibition of photosynthetic apparatus of cyanobacteria [26]. Note that histograms $P(\Delta h)$ for CCCP- or KCN-treated cyanobacteria were virtually independent of cell exposure to light (data not shown). Summing up results of experiments outlined above, we conclude that optical parameter Δh of a topogram can be considered as a measure of metabolic activity in single cyanobacterial cells.

As we noted above, a phase thickness $\Delta h(x,y)$ depends on the product of the local refractive index of the object, $\Delta n(x,y)$, and its geometrical size in Z-direction [17]. Comparison of histograms $P(\Delta h)$ and $P(d)$ (Fig. 5) demonstrate that a rather broader profile $P(\Delta h)$ in a population of control cells cannot be attributed entirely to significant variations of geometrical sizes in control cells. Actually, cell treatment either with an uncoupler CCCP or with inhibitors (KCN or DCMU) did not influence an average diameter of cells ($\langle d \rangle \approx 1.8-1.9$ μm) (Fig. 5a). In the meantime, the profile $P(\Delta h)$ narrowed substantially with inhibition of cell metabolic activity (Fig. 5b). Fig. 5c shows histograms $P(\Delta n)$ plotted for normalized phase thickness $\Delta n = \Delta h/d$. Parameter Δn may be regarded as a difference ($\Delta n = \langle n \rangle - n_o$) of the refractive indices of an object and that of an immersion solution n_o [17]. If we assume that the cell size along Z-axis is proportional to the cell diameter d, then Δn should be determined mainly by refractive index rather than by geometrical height of a sample. For intact cells, the profile of $P(\Delta n)$ (Fig. 5c) was broader than in populations of inhibitor-treated cells. This observation means that the population of control cells included a subpopulation with relatively high values Δn ($\Delta n \geq 0.05$) that was not observed in inhibitor-treated cells. Thus, we can conclude that both optical parameters, Δh and Δn, can serve as a measure of cell metabolic activity.

3.2. Spores Bacillus licheniformis

We also came to the conclusion that optical parameters Δh and Δn reflect metabolic activity comparing CPM images (Fig. 6a) and distributions of parameters d and Δh in control (dormant) and inactivated (thermally-treated) populations of spores *Bacillus licheniformis* (Fig. 6b). Profiles of histograms $P(d)$ are certainly different (Fig. 6c, d), however, the mean values of diameter d for both groups, control and inactivated, are close ($\langle d \rangle \approx 1$ μm). In the meantime, the control group of spores is characterized by much higher phase thickness (Fig. 6e, $\langle \Delta h \rangle \approx 80$ nm) than inactivated spores (Fig. 6f, $\langle \Delta h \rangle \approx 25$ nm).

The effect described above, i.e., a decrease in the phase height Δh and averaged refractive index Δn caused by suppression of a cell metabolic activity, is likely to be a rather general phenomenon. Dependence of Δh on energ-

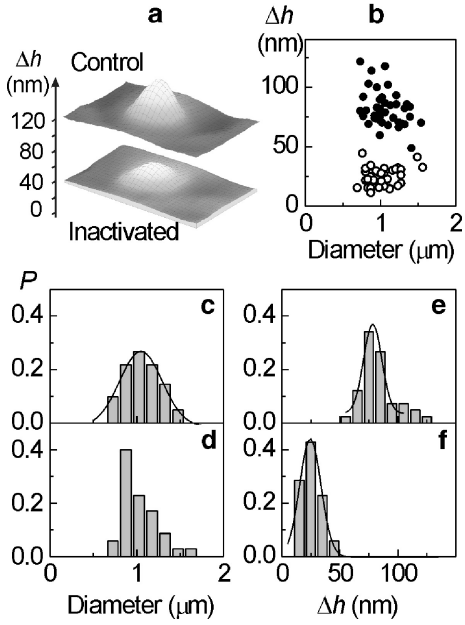

Fig. 6. Experimental results showing the dependence of a CPM image on the functional state of spores of *Bacillus licheniformis*. (a) 3D images of control and inactivated spores. Control (dormant) spores were suspended in distilled water and then viewed microscopically for measurements. Inactivated samples were prepared by heating spores for 20 min at 115 °C. (b) Plots Δh versus d for populations of control spores (solid circles, $N=41$) and inactivated spores (open circles, $N=35$). (c–f) Histograms demonstrating spores distribution over diameter d (c, d) and phase thickness Δh (e, f) for populations of control (c, e) and inactivated (d, f) spores.

ization of coupling membrane has been demonstrated for isolated energy transducing organelles, mitochondria [18,19] and chloroplasts [20]. There may be different reasons for variability of Δh; for instance, phase thickness could be sensitive to structural changes in biomembranes or to spectral changes in intracellular pigments caused by shifts in the redox status of electron carriers. Results of our experiments with cyanobacteria indicate, however, that a decrease in Δh could not be attributed entirely to spectral shifts. Actually, uncouplers and inhibitors of electron transport should cause opposite effects on the redox state of electron carriers in cyanobacteria [21], whereas we observed that addition of an uncoupler CCCP and inhibitors (KCN or DCMU) caused similar effect on Δh value (Fig. 4). A correlation between the phase thickness Δh and metabolic states of isolated mitochondria was interpreted in terms of the membrane electro-optical effect [17–19], that is, a dependence of the membrane refractive index on the transmembrane difference in electric potentials. Inhibition of mitochondrial respiratory chain by rotenone caused a decrease in the $<\Delta n>$ value from 0.05–0.07 to 0.025. Taking together, our results demonstrate that CPM images of single cells and intracellular organelles are sensitive to variations of their metabolic states. Metabolically active specimens are characterized by higher phase thicknesses Δh than de-energized (or "dead") ones.

Acknowledgements

This work was partly supported by grants from the Russian Foundation for Basic Researches (grants 03-04-48981 and 04-04-49132), INTAS (grant 01-483), and Program "Universities of Russia". The authors are grateful to Dr. O.A. Koksharova for the supply of cyanobacteria cells, Dr. Yu.A. Nikolaev for the supply of spores and fruitful discussions, and Dr. S.K. Chamorovsky for critical reading the manuscript.

References

[1] D.E. Olins, A.L. Olins, H.A. Levy, R.C. Durfee, S.M. Margle, E.P. Tinnel, S.D. Dover, Electron microscope tomography: transcription in three dimensions, Science 220 (1983) 498–500.
[2] J.R. McIntosh, Electron microscopy of cells: a new beginning for a new century, J. Cell Biol. 153 (2001) F25–F32.
[3] W. Baumeister, Electron tomography: towards visualization the molecular organization of the cytoplasm, Curr. Opin. Struct. Biol. 12 (2002) 679–684.
[4] A.J. Koster, J. Klumperman, Electron microscopy in cell biology: integrating structure and function, Nat. Rev., Mol. Cell Biol. 4 (2003) SS6–SS10.
[5] D. Gerlich, J. Ellenberg, 4D imaging to assay complex dynamics in live specimens, Nat. Cell Biol. 5 (2003) S14–S19.
[6] J.B. Pawley (Ed.), Handbook of Biological Confocal Microscopy, Plenum Press, New York, 1995.
[7] C.W. Mullineaux, M. Sarcina, Probing the dynamics of photosynthetic membranes with fluorescence recovery after photobleaching, Trends Plant Sci. 7 (2002) 237–240.
[8] H. Noji, R. Yasuda, M. Yoshida, K. Kinosita Jr., Direct observation of the rotation of F1-ATPase, Nature 386 (1997) 299–302.
[9] J. Lippincott-Schwartz, N. Altan-Bonnet, G.H. Patterson, Photobleaching and photoactivation: following protein dynamics in living cells, Nature Cell Biol. 5 (2003) S7–S14.
[10] J. White, E. Steizer, Photobleaching GFP reveals protein dynamics inside live cells, Trends Cell Biol. 9 (1999) 61–65.
[11] A. Miyawaki, A. Sawano, T. Kogure, Lighting up cells: labeling proteins with fluorophores, Nat. Cell Biol. 5 (2003) S1–S7.
[12] J. Lippincott-Schwartz, G.H. Patterson, Development and use of fluorescent protein markers in living cells, Science 300 (2003) 87–91.
[13] V.P. Skulachev, Mitochondrial filaments and clusters as intracellular power-transmitting cables, Trends Biochem. Sci. 26 (2001) 23–29.
[14] M.A. Aon, S. Cortassa, B. O'Rourke, Percolation and criticality in a mitochondrial network, Proc. Natl Acad. Sci. U. S. A. 101 (2004) 4447–4452.
[15] M. Teuber, M. Rögner, S. Berry, Fluorescent probes for non-invasive bioenergetic studies of whole cyanobacterial cells, Biochim. Biophys. Acta 1506 (2001) 31–46.
[16] M.F. Cano Abad, G. Di Benedetto, P.J. Magalha, L. Filippin, T. Pozzan, Mitochondrial pH monitored by a new engineered green fluorescent protein mutant, J. Biol. Chem. 279 (2004) 11521–11529.
[17] V.P. Tychinsky, Coherent phase microscopy of intracellular processes, Physics Uspekhi 44 (2001) 617–629.
[18] V.P. Tychinsky, D. Weiss, T.V. Vyshenskaya, L.S. Yaguzhinsky, S.L. Nikandrov, Cooperative processes in mitochondria: measurement by dynamic phase microscopy, Biofizika (Biophysics) 45 (2000) 870–877.
[19] V. Tychinsky, A. Kretushev, T. Vyshenskaya, Mitochondria optical parameters are dependent on their energy state: a new electrooptical effect? Eur. Biophys. J. 33 (2004) 700–705.
[20] V.P. Tychinsky, A.V. Kretushev, T.V. Vyshenskaya, A.N. Tikhonov, A dynamic phase microscopic study of optical characteristics of individual chloroplasts, Biochim. Biophys. Acta 1665 (2004) 57–64.
[21] B.V. Trubitsin, M.D. Mamedov, L.A. Vitukhnovskaya, A.Yu. Semenov, A.N. Tikhonov, EPR study of photosynthetic electron transport control in cells of *Synechocystis* sp. strain PCC 6803, FEBS Lett. 544 (2003) 15–20.
[22] I. Barak, E. Ricca, S.M. Cutting, From fundamental studies of sporulation to applied spore research, Mol. Microbiol. 55 (2005) 330–338.
[23] J.J. van Thor, R. Jeanjean, M. Havaux, K.A. Sjollema, F. Joset, K.J. Hellingwerf, H.C.P. Matthijs, Salt shock-inducible Photosystem I cyclic electron transfer in Synechocystis PCC 6803 relies on binding of ferredoxin: $NADP^+$ reductase to the thylakoid membranes via its CpcD phycobilisome-linker homologous N-terminal domain, Biochim. Biophys. Acta 1457 (2000) 129–144.
[24] V.P. Skulachev, Membrane Bioenergetics, Springer-Verlag, Berlin, 1988.
[25] A. Trebst, Inhibitors in electron flow: tools for the functional and structural localization of carriers and energy conservation sites, Methods Enzymol. 69 (1980) 675–715.
[26] A. Melis, Photosystem-II damage and repair cycle in chloroplasts: what modulates the rate of photodamage in vivo? Trends Plant Sci. 4 (1999) 130–135.